Positron scattering from rare gases (He, Ne, Ar, Kr, Xe, and Rn): Total cross sections at intermediate and high energies

K. L. Baluja* and Ashok Jain
Physics Department, Florida A&M University, Tallahassee, Florida 32307
and Supercomputer Computations Research Institute, Florida State University, Tallahassee, Florida 32304
(Received 16 December 1991)

The total (elastic plus inelastic) cross sections for positron scattering from all the rare gases are reported at intermediate and high energies (20–1000 eV), where experimental data are available for comparison except for the case of radon gas. A complex-optical-potential [$V_{opt}(r)$] approach is employed in which the real part (static plus polarization terms) is calculated from Hartree-Fock or Dirac-Hartree-Fock target wave functions. The imaginary part of the optical potential, i.e., the absorption potential [$V^{+}_{abs}(r)$], is derived for each gas semiempirically from the corresponding electron absorption potential [$V^{-}_{abs}(r)$] in the form of $V^{+}_{abs}(r)=f(k,r)V^{-}_{abs}(r)$, where $f(k,r)$ depends on the incident energy (k^2) and radial distance (r). The V^{-}_{abs} is taken from the work of Truhlar and co-workers. The $V_{opt}(r)$ is treated exactly in a partial-wave analysis under the variable-phase method. With the present form of $V_{opt}(r)$, we are able to reproduce experimental σ_t values at all energies considered here. An additional feature of the present results is that the inelastic cross sections compare very well with the measured inelastic (sum of positronium formation, excitation, and ionization cross sections) values for rare gases, where such experimental data are available. The σ_t for the positron-Rn system are predicted. We also discuss the correlation between scattering cross section and the atomic properties. We found that at intermediate and high energies, the positron-gas total cross section can be represented by an analytic formula $\sigma_t(10^{-16}\ \mathrm{cm}^2)=21.16\sqrt{\alpha_0(a_0^3)/E(\mathrm{eV})}$, where α_0 is the target polarizability and E is the impact energy. This simple form of the σ_t in terms of target polarizability works very well for highly polarizable targets such as the alkali-metal atoms and several hydrocarbon molecules. In particular, by using the above analytic formula for σ_t, we have shown that our results for Na, K, Rb, C_2H_4, C_2H_6, and C_3H_6 targets compare very well with the experimental data.

PACS number(s): 34.80.−i, 34.90.+q, 61.80.Fe

I. INTRODUCTION

The total cross sections (σ_t) (including elastic plus all energetically possible inelastic channels) for positron–rare-gas collisions have been measured from the low ($\sim$1 eV) to keV energy region by a number of investigators during a period of the past two decades (see Refs. [1–26]). Several review articles [27–35] have summarized the experimental progress and the data on the positron scattering total cross sections from low to intermediate and high energies. In this paper we are concerned only with intermediate and high energies (20–1000 eV) where very little theoretical work has been done (see Table I). Only a few calculations are available on the total cross sections for positron-He, -Ne, and -Ar collisions at and above 100-eV energy (see Refs. [36–46]). No calculations on the σ_t are available for the positron-Kr, -Xe, and -Rn systems. In addition, the theoretical work on these gases between 20–100 eV is almost negligible. From this point of view, there is a need to perform theoretical calculations on the positron-atom total cross sections in the present energy region. At low energies ($E \leq 20$ eV), a proper close-coupling scheme is suitable. However, a most difficult energy regime is between E_{Ps} and 20 eV (here E_{Ps} is the threshold for positronium formation), where the coupling between various inelastic channels, including the positronium (Ps) formation one, is very difficult to include for many-electron targets.

In the present intermediate and high energies ($E \geq 20$ eV), all the inelastic rearrangement channels (Ps formation, excitation, and ionization) are open (except for He) and therefore a proper *ab initio* calculation is almost impossible. It is thus quite obvious that most of the calculations carried out so far on the positron-atomic systems have been restricted to below the E_{Ps} energy only. At and above 100 eV, several high-energy approximations have been employed for He, Ne, and Ar gases (see the reviews in Refs. [47,48]). For example, the eikonal-Born series (EBS) theory of Byron and Joachain [38], optical model approximation of EBS theory [39], distorted-wave second-order Born (DWSB) approximation [37], and modified versions of Glauber theory [41] (for a general review see Ref. [48]). The only intermediate-energy (1–100 eV) calculations on the σ_t for Ne and Ar systems are due to Bartschat, McEachran, and Stauffer [45,46], who employed an optical-potential method, quite similar to the present one except for the choice of optical potential; however, due to the neglect of ionization and Ps formation channels in the evaluation of optical potential, their σ_t values are too low in comparison to the experimental data (see later). It is rather disappointing that very little

TABLE I. Summary of total cross sections (σ_t) available in the literature for positron scattering with rare gases. Note that the low-energy (below 20 eV) calculations are excluded from the following bibliography.

	Energy range (eV)	
Rare gas	Expt. Data	Theory
He	1–4, 17–26 [1]; 2–20 [2]; 4–19 [3]; 2–400 [4]; 4–E_{Ps} [5] 19–27 [7]; 16–270 [9]; 50–400 [10]; 2–960 [12]; 2–18 [14] 0.3–31 [16]; 1–6 [17]; 2–50 [18]; 20–1000 [19]; 15–800 [23] 0.6–22 [26]	100–3000 [37]; 100–500 [38] 100–700 [39]; 50–1000 [41]
Ne	2–400 [4]; 4–E_{Ps} [5]; 4–14 [6]; 15–272.5 [11]; 2–960 [12] 20–1000 [15]; 0.25–24 [16]; 2–50 [18]; 50–800 [19] 1–6 [22]; 15–800 [23]	200–3000 [37]; 100–500 [38] 100–800 [42]; 1–100 [46]
Ar	8 [2]; 2–400 [4]; 4–E_{Ps} [5]; 4–14 [6]; 25–300 [11] 2–960 [12]; 0.4–18 [13]; 200–1000 [15]; 20–800 [19] 2–50 [20]; 1–6 [22]; 15–800 [23]	100–1000 [40]; 100–800 [43] 3–300 [44]; 1–100 [45]
Kr	2–400 [4]; 200–960 [12]; 0.35–100 [21]; 1–6 [22] 20–800 [24]	none
Xe	2–400 [8]; 2–50 [20]; 0.35–100 [21]; 1–6 [22]; 20–800 [24]	none
Rn	none	none

attention has been paid theoretically to determine total cross section for positron-atom scattering at intermediate and high energies.

Our goal in this paper is to present σ_t values for all the rare gases in a wide energy region (20–1000 eV). Finally, the calculated σ_t are fitted to a simple formula [$\sigma_t = c(\alpha_0/E)^{1/2}$, where c is a constant, α_0 is the polarizability of the target in atomic units, and E is the impact energy in eV]. This form of σ_t works very well for all the rare gases (except for the He and Ne gases, see later), alkali-metal atoms (for example, Na, K, and Rb atoms where recent experimental data [49] on the σ_t are available), and a large number of molecules [50]. We also discuss the correlation between σ_t and α_0 and compare our analysis with a similar correlation study by Szmytkowski [35].

In the present method, the total cross section is the sum of elastic (σ_{el}) and absorption (σ_{abs}) terms. The σ_{abs} quantity represents the sum of all possible inelastic channels (excitation, ionization, and positronium formation, i.e., $\sigma_{abs}=\sigma_{ion}+\sigma_{Ps}+\sigma_{exc}$). The σ_{ion} cross section constitutes nearly more than half of the corresponding σ_t for almost all the atomic and molecular targets [51]. Thus it is possible to make a satisfactory estimate of σ_{ion} for a given target from the present theory. Some examples are presented for the He and Kr cases where σ_{ion} and σ_{Ps} cross sections for the positron scattering have been measured recently. We also present our σ_{el} results for all the gases in the present energy regime and compare σ_{el} for the positron-He case where recent experimental numbers are available.

In the next section, we provide theoretical details, while in Sec. III numerical procedure and results are discussed. The correlation of σ_t with molecular parameters is analyzed in Sec. IV. The concluding remarks are made in the final section, Sec. V. We use atomic units in this paper until otherwise specified.

II. THEORY

The basic Schrödinger equation of the positron-atom system is given by

$$(\hat{H}_T+\hat{V}_{\text{int}}+E)\Psi_T(\mathbf{r}_1,\ldots,\mathbf{r}_N,\mathbf{r})=0 \ . \tag{1}$$

The total wave function of the N target electrons ($\mathbf{r}_N$) and projectile ($\mathbf{r}$) can be written in a close-coupling scheme as

$$\Psi_T^{LS\pi}(\mathbf{r}_1,\ldots,\mathbf{r}_N;\mathbf{r})=\sum_i \Phi_i^{LS\pi}(\mathbf{r}_1,\ldots,\mathbf{r}_N;\hat{\mathbf{r}})\frac{1}{r}F_i(r) \ . \tag{2}$$

In Eq. (2), we have a sum over all discrete target states including an integration over all continuum space. The channel functions $\Phi_i^{LS\pi}$, with total angular momentum L, total spin S, and total parity π are obtained by coupling the angular momenta of target and projectile. In a standard close-coupling treatment, the N-electron target Hamiltonian of the system,

$$\hat{H}_T=\sum_{i=1}^{N}-\tfrac{1}{2}\nabla_i^2-\frac{Z}{r_i}+\tfrac{1}{2}\sum_{i,j=1}^{N}\frac{1}{|\mathbf{r}_i-\mathbf{r}_j|} \ , \tag{3}$$

is diagonalized under the channel functions [Eq. (2)] to give a set of coupled equations for the projectile continuum function $F_i(r)$, as

$$\left[\frac{d^2}{dr^2}-\frac{l_i(l_i+1)}{r^2}+k_i^2\right]F_i(r)=2\sum_j U_{ij}(r)F_j(r) \ , \tag{4}$$

where the potential coupling term is given by

$$U_{ij}(r)=\frac{Z}{r}\delta_{ij}-\sum_{k=1}^{N}\left\langle\Phi_i\left|\frac{1}{\mathbf{r}_k-\mathbf{r}}\right|\Phi_j\right\rangle \ . \tag{5}$$

In the above close-coupling formulation, the sum has to be truncated with only a few target states, which is feasible only at low impact energies. However, at inter-

mediate and high energies, it is not possible to solve Eq. (4) as such with a large number of discrete and continuum states. A convenient way to deal with this problem is to mimic the effects of excited target states including the ionization (and Ps formation channel too) process via a local optical-potential approach [52]. Thus the scattering Eq. (4) can be approximated to

$$\left[\frac{d^2}{dr^2}-\frac{l(l+1)}{r^2}+k^2-2V_{\rm opt}(r)\right]F(r)=0\ . \tag{6}$$

The optical potential in Eq. (6) takes care of closed and open channels. It becomes complex when open channels are involved in the collision, which is the case in the present energy range. The imaginary part of $V_{\rm opt}(r)$ takes into account the loss of flux due to all energetically possible inelastic channels, while the real part represents the target polarization effects. In general, the optical potential is energy dependent. The optical potential, $V_{\rm opt}(r)=V_{\rm st}(r)+V_{\rm pol}(r)+iV_{\rm abs}(r)$, is very difficult to determine from *ab initio* methods. Byron and Joachain [47] (see also Ref. [48]) have discussed various methods to compute $V_{\rm opt}(r)$ from first principles. However, in their calculation at the second-order level only, the computed $V_{\rm opt}(r)$ for a few rare gases (He, Ne, and Ar) is the same for electron and positron projectiles. In the present positron calculations, we employ approximate local $V_{\rm pol}(r)$ and $V_{\rm abs}(r)$ potentials which are quite different from the corresponding electron potentials.

The repulsive static potential $V_{\rm st}(r)$ is calculated from the unperturbed target wave function Φ_0 at the Hartree-Fock level (see later). For heavier targets (Kr, Xe, and Rn), we employ relativistic charge density and relativistic static potential (see later), which is essential due to contraction of the target because of relativistic effects. Here, we determine the $V_{\rm pol}(r)$ in the positron correlation-polarization (PCOP) approximation recently proposed by one of the authors [53–55]. The PCOP potential is based on the correlation energy $\varepsilon_{\rm corr}(r_s)$ (where r_s is the density parameter), of a single positron in a homogeneous electron gas. Thus the PCOP polarization potential $V_{\rm pol}^{\rm PCOP}(r)$ for the positron-atom system is given by

$$V_{\rm pol}^{\rm PCOP}(r)=\begin{cases} V_{\rm corr}(r), & r\le r_c \quad (7a)\\ -\dfrac{\alpha_0}{2r^4}, & r\ge r_c \quad (7b)\end{cases}$$

where r_c is the radius where the $V_{\rm corr}(r)$ and $-\alpha_0/2r^4$ terms cross each other for the first time. The $V_{\rm corr}(r)$ in Eq. (7a) is given as (in atomic units), for $r_s\le 0.302$,

$$2V_{\rm corr}(r)=\frac{-1.82}{(r_s)^{1/2}}+[0.051\ln(r_s)-0.115]\times\ln(r_s)+1.167\ ; \tag{8a}$$

for $0.302\le r_s\le 0.56$,

$$2V_{\rm corr}(r)=-0.923\,05-\frac{0.090\,98}{r_s^2}\ ; \tag{8b}$$

and for $0.56\le r_s\le 8.0$,

$$2V_{\rm corr}(r)=-\frac{8.7674r_s}{(r_s+2.5)^3}+\frac{-13.151+0.9552r_s}{(r_s+2.5)^2}+\frac{2.8655}{(r_s+2.5)}-0.6298\ , \tag{8c}$$

where the density parameter r_s is given by

$$\tfrac{4}{3}\pi r_s^3\rho(r)=1\ , \tag{9}$$

with $\rho(r)$ being the target undistorted electronic density. In Eqs. (8a)–(8c) we do not worry about the $8.0\le r_s\le\infty$ region, as this range is beyond the crossing point where the polarization potential is accurately described by the $-\alpha_0/2r^4$ term.

For the calculation of $V_{\rm abs}(r)$, we employ a local absorption potential derived semiempirically from the electron absorption potential $[V_{\rm abs}^{-}(r)]$ of Truhlar and coworkers [56]. The $V_{\rm abs}^{-}(r)$ is a function of molecular charge density, incident electron energy, and the mean excitation energy Δ of the target. The absorption ($\sigma_{\rm abs}$) and the σ_t cross sections depend significantly on the choice of the value of Δ. The final form of the present positron absorption interaction $[V_{\rm abs}^{+}(r)]$ is determined approximately which is different for different targets. In brief, the $V_{\rm abs}^{+}(r)$ is derived from the corresponding $V_{\rm abs}^{-}(r)$ as follows:

$$V_{\rm abs}^{+}(r)=f(k,r)V_{\rm abs}^{-}(r)\ . \tag{10}$$

The form of $f(k,r)$ is given in Table II along with other parameters of rare gases. The $V_{\rm abs}^{-}$ in Eq. (10) is given by [56]

$$V_{\rm abs}^{-}(r)=-\rho(r)(v_{\rm loc}/2)^{1/2}(8\pi/5k^2k_f^3)\times H(k^2-k_f^2-2\Delta)(A_1+A_2+A_3)\ , \tag{11}$$

TABLE II. Rare-gas parameters (for details see the text).

Molecule	α_0 (units of a_0^3)	IP (eV)	$E_{\rm Ps}$ (eV)	Δ (eV)	$f(k,r)$ [Eq. (11)]
He	1.38	24.59	17.79	14.0	$2/kr$
Ne	2.67	21.56	14.76	12.0	$2/kr$
Ar	11.08	15.60	8.80	7.0	$2/\sqrt{kr}$
Kr	16.76	14.00	7.20	6.0	$2/\sqrt{kr}$
Xe	27.29	12.13	5.33	5.0	$2/\sqrt{kr}$
Rn	35.77	10.75	3.95	3.95	$2/\sqrt{kr}$

where

$$v_{\rm loc}(r)=k^2-V_{\rm st}(r)-V_{\rm ex}(r)-V_{\rm pol}\ , \tag{12a}$$

$$A_1=5k_f^3/2\Delta\ , \tag{12b}$$

$$A_2=-k_f^3(5k^2-3k_f^2)/(k^2-k_f^2)^2\ , \tag{12c}$$

$$A_3=2H(2k_f^2+2\Delta-k^2)\frac{(2k_f^2+2\Delta-k^2)^{5/2}}{(k^2-k_f^2)^2}\ , \tag{12d}$$

where $\frac{1}{2}k^2$ is the energy of the incident electron in hartrees. Here $H(x)$ is a Heaviside function defined by $H(x)=1$, for $x\geq 0$ and $H(x)=0$ for $x<0$. In the present positron case, $V_{\rm ex}(r)$ is zero and $V_{\rm st}(r)$ is repulsive. By varying the value of Δ in $V_{\rm abs}^-(r)$ one can improve the absorption ($\sigma_{\rm abs}$) or σ_t cross sections relative to experimental or more accurate *ab initio* calculations.

After generating the full optical potential of a given positron-atom system, we treat it exactly in a partial-wave analysis by converting Eq. (6) in terms of the following set of first-order coupled differential equations for the real (χ_l) and imaginary ($\bar{\chi}_l$) parts of the complex phase-shift function under the variable-phase approach (VPA) [57],

$$\chi_l'(kr)=-\frac{2}{k}\{2[V_{\rm st}(r)+V_{\rm pol}(r)](A^2-B^2) +2V_{\rm abs}^+(r)AB\}\ , \tag{13}$$

$$\bar{\chi}_l'(kr)=-\frac{2}{k}\{2[V_{\rm st}(r)+V_{\rm pol}(r)]AB -2V_{\rm abs}^+(r)(A^2-B^2)\}\ , \tag{14}$$

where

$$A=\cosh\bar{\chi}_l(kr)[\cos\chi_l(kr)j_l(kr)-\sin\chi_l(kr)\eta_l(kr)]\ , \tag{15a}$$

$$B=-\sinh\bar{\chi}_l(kr)[\sin\chi_l(kr)j_l(kr)-\cos\chi_l(kr)\eta_l(kr)]\ , \tag{15b}$$

and $j_l(kr)$ and $\eta_l(kr)$ are the usual Riccati-Bessel functions [57]. Equations (13) and (14) are integrated up to a sufficiently large r different for different l and k values. Thus the final S matrix is written as

$$S_l(k)=\exp(-2\bar{\chi}_l)\exp(i2\chi_l)\ . \tag{16}$$

The integrated elastic ($\sigma_{\rm el}$), $\sigma_{\rm abs}$, and σ_t cross sections are described in terms of the S matrix as follows:

$$\sigma_{\rm el}^l=\frac{\pi}{k^2}(2l+1)|1-S_l(k)|^2,\quad \sigma_{\rm el}=\sum_{l=0}^{l_{\max}}\sigma_{\rm el}^l\ , \tag{17}$$

$$\sigma_{\rm abs}^l=\frac{\pi}{k^2}(2l+1)[1-|S_l(k)|^2],\quad \sigma_{\rm abs}=\sum_{l=0}^{l_{\max}}\sigma_{\rm abs}^l\ , \tag{18}$$

$$\sigma_t^l=\frac{2\pi}{k^2}(2l+1)[1-{\rm Re}S_l(k)],\quad \sigma_t=\sum_{l=0}^{l_{\max}}\sigma_t^l\ . \tag{19}$$

We note that $\sigma_t=\sigma_{\rm el}+\sigma_{\rm abs}$.

III. RESULTS AND DISCUSSION

A. Numerical details

In order to evaluate the optical potential for Eq. (6), we need target charge density as the basic input. The corresponding charge density and the static potential are calculated from the unperturbed charge density $\rho(r)$ of the atom which is obtained from a self-consistent method of Froese-Fischer [58] (for more details see also Jain, Etemadi, and Karim [59]). For heavier gases (Kr, Xe, and Rn) we employ relativistic description of target charge density [$\rho(r)$] and relativistic static interaction computed in the Dirac-Hartree-Fock-Slater (DHFS) scheme due to Salvat *et al.* [60]. In this scheme, the one-electron orbitals are the solutions of the Dirac equation instead of the Schrödinger equation. This incorporates relativistic effects in a natural way. Salvat *et al.* [60] parametrized the DHFS atomic screening function and expressed the $\rho(r)$ and $V_{\rm st}(r)$ in convenient analytic forms as follows:

$$\rho(r)=\frac{Z}{4\pi r}\sum_{i=1}^{3}A_i\alpha_i^2e^{-\alpha_i r}\ , \tag{20}$$

$$V_{\rm st}(r)=\frac{Z}{r}\sum_{i=1}^{3}A_ie^{-\alpha_i r}\ , \tag{21}$$

where A_i and α_i are the parameters with the imposed condition $\sum_{i=1}^3 A_i=1$. However, for Kr and Xe atoms there are only three independent parameters, namely, A_1, α_1, and α_2 (note that the fourth parameter A_2 as listed below is given by the relation $A_1+A_2=1$). For Kr, Xe, and Rn atoms, these parameters are given as [60]

Kr: $A_1=0.4190$, $A_2=0.5810$,
$\alpha_1=9.9142$, $\alpha_2=1.8835$,

Xe: $A_1=0.4451$, $A_2=0.5549$,
$\alpha_1=11.805$, $\alpha_2=1.7967$,

Rn: $A_1=0.0955$, $A_2=0.6060$, $A_3=0.2985$,
$\alpha_1=43.489$, $\alpha_2=5.852$, $\alpha_3=1.5736$.

In order to solve Eqs. (13) and (14), we need a large number of partial waves [$l_{\max}$ in Eqs. (17)–(19)] in the present intermediate- and high-energy region. We carried out convergence tests with respect to radial distance and the step size to preserve numerical accuracy. The value of $l_{\max}$ varied from 20 to 400 depending upon the impact energy. The $V_{\rm abs}^+$ is a short-range potential and does not require more than 30 partial waves at the highest energy of the present energy region. In Table II, we have provided the values of $E_{\rm Ps}$ and α_0 parameters for each rare gas studied in this paper.

B. Justification of the choice of $V_{\rm abs}^+(r)$ in Eq. (10)

The justification of choosing $V_{\rm abs}^+(r)$ in terms of $V_{\rm abs}^-(r)$ [Eq. (10)] comes from the following argument: The $V_{\rm abs}^-(r)$ is a function of target charge density, projectile energy, Fermi momentum, mean excitation energy, etc.

It is also a well-known fact that evaluation of $V^{-}_{abs}(r)$ is a very difficult problem from an *ab initio* point of view. For the present positron case, $V^{-}_{abs}(r)$ is different from the corresponding electron case since the $V_{ex}(r)$ (exchange potential) is zero and the $V_{st}(r)$ (static potential) is repulsive. In the original derivation of $V^{-}_{abs}(r)$ (see Ref. [56]), the imposed conditions that (i) the initially unbound electron is not allowed to fall into the occupied Fermi sea, and (ii) the lowest-energy state is available to the initially bound electron exceeds the Fermi level by the energy gap (Δ), are also valid for the present positron scattering. Also note that a factor of $\frac{1}{2}$ that approximately accounts for the exchange interaction in the original derivation of $V^{-}_{abs}(r)$ (see Ref. [56]), is removed in the present calculation of $V^{-}_{abs}(r)$ for the positron in Eq. (10). Thus the choice of $V^{+}_{abs}(r)$ in terms of $V^{-}_{abs}(r)$ is fully justified [note that actual numerical values of $V^{-}_{abs}(r)$ for electron and positron are different]. Also we do not know the actual relationship between $V^{+}_{abs}(r)$ and $V^{-}_{abs}(r)$, therefore a simple relationship [Eq. (10)] assumed in this work, can only be justified by its success in reproducing experimental data for a large number of targets as will be demonstrated below. In addition, we have found that form [Eq. (10)] gives a good comparison of $V^{+}_{abs}(r)$ for rare gases between present results and the calculation of Joachain and Potvliege [61].

The positron-atom total cross sections are generally characterized by a sharp rise near the Ps threshold and a bell-shaped structure around 20–80 eV depending upon the corresponding target. It is therefore very important to reproduce the shape of the observed σ_t in a theoretical model. This has been the main criterion to find the unknown function $f(k,r)$ in Eq. (10). In order to further justify the choice of Eq. (10), we can argue that (1) the $V^{+}_{abs}(r)$ must be quite different from the corresponding $V^{-}_{abs}(r)$; (2) a proper form of $V^{+}_{abs}(r)$ should reproduce all salient features in positron σ_t behavior as a function of impact energy; (3) the individual components (σ_{el}, σ_{abs}) should be meaningful when compared with other data, experimental or theoretical; and finally (4) it is very difficult to determine $V^{+}_{abs}(r)$ *ab initio* even for the simplest few-electron targets.

C. Total (σ_t) cross sections for He, Ne, Ar, Kr, Xe, and Rn

Figure 1 displays our positron-He σ_t values at 20–1000 eV along with experimental points from Dutton, Harris, and Jones [10], Stein *et al.* [16], Griffith *et al.* [19], and Kauppila *et al.* [23]. We have not shown experimental error bars which are around 15%. We can see a very good agreement between present theory and the measurements at all energies (20–1000 eV) except near the peak, where our results are about 15% higher than the experimental values. However, around the peak, the measurements of Dutton, Harris, and Jones [10] are much higher as compared to other experimental data and the present theory. In Fig. 1 we have also shown previous calculations [37,38] available at and above 100 eV. The optical model calculations of Byron and Joachain [38] seem to be better than the DWSB results of Dewangen and Walters [37]. In Fig. 1, we have also plotted the Bethe-Born [62–64] results which are the same for both the electrons and positrons. Our solid curve (Fig. 1) presents very good comparison with experimental data (in shape and magnitude both) in a wide energy range, while the previous calculations, available above 100 eV only, do not cover the whole range of intermediate- and high-energy regions.

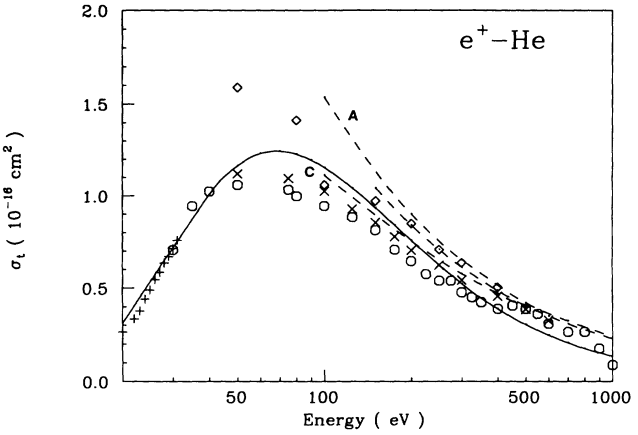

FIG. 1. Total cross sections for the positron-He scattering at 20–1000 eV. Theory: solid curve, present results; curve *A*, second-order Born calculations of Ref. [37]; curve *B*, Bethe-Born results of Inokuti and co-workers (Refs. [62,63]); curve *C*, optical model results of Ref. [38]. The experimental points are from Ref. [23] (×), [19] (○), [16] (+), and [10] (◇).

The positron-Ne σ_t are shown in Fig. 2 along with

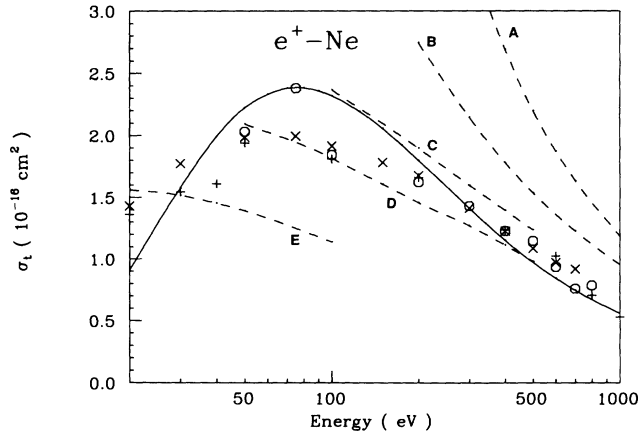

FIG. 2. Total cross sections for the positron-Ne scattering in the range 20–1000 eV. Calculations: solid line, present results; dashed curve *A*, Born-Bethe theory (Refs. [62,63]); dashed curve *B*, second-order Born calculations of Ref. [37]; dashed curve *C*, optical model theory of Ref. [38]; dashed curve *D*, calculations of Ref. [42]; dashed curve *E*, calculations of Ref. [46]. Experimental data: ×, Kauppila *et al.* (Ref. [23]); +, Brenton, Dutton, and Harris (Ref. [15]); ○, Griffith *et al.* (Ref. [19]).

selected (see Table I) measurements of Brenton, Dutton, and Harris [15], Griffith *et al.* [19], and Kauppila *et al.* [23]. Again we see that there is an overall agreement between present theory and all these observations; however, we should also realize that there is considerable discrepancy between the measurements of Kauppila *et al.* [23] and Brenton, Dutton, and Harris [15]. Around the peak (70 eV), all three measurements have significant deviation from each other. On the other hand, the situation with previous calculations is not very good. In Fig. 2, we have included several calculations for comparison with present theory and experimental data. Only the optical model results of Byron and Joachain [38] (100–500 eV, dashed curve *C*) and calculations of Lata [42] (50–500 eV, dashed curve *D*) are in fair accord with measured points. The DWSB calculations of Dewangan and Walters [37] (200–3000 eV, dashed curve *B*) are too high, while the Born-Bethe theory (dashed curve *A*) totally fails for this system in the present energy region. The optical-potential calculations of Bartschat, McEachran, and Stauffer [46] (20–100 eV, dashed curve *E*) are very poor with the incorrect shape and magnitude both for the energy dependence of σ_t. The poor agreement between results of Bartschat, McEachran, and Stauffer [46] and the experiment is mainly because of the neglect of ionization channel in their optical-potential model. Our total cross-section values clearly reproduce the hump structure around 75 eV.

Our positron-Ar total cross sections are depicted in Fig. 3 along with experimental data of Kauppila *et al.* [23] (15–800 eV, crosses), Brenton, Dutton, and Harris [15] (200–1000 eV, +) and Griffith *et al.* [19] (20–800 eV, open circles). All these experimental results (in Fig. 3) clearly reveal a peaking structure around 45 eV which is also present in our calculations (full curve in Fig. 3). The agreement between our results and all these measurements included in Fig. 3 is within experimental uncertainty (not shown). In Fig. 3 we have also included previous theoretical calculations. As was the case in positron-Ne scattering (see Fig. 2), the optical-potential calculations (20–100 eV, dashed curve *D*) of Bartschat, McEachran, and Stauffer [45] are too low, again due to insufficient inclusion of inelastic channels (particularly the ionization process). The high-energy optical model calculations of Joachain *et al.* [40] (100–500 eV, dashed curve *C*) and complex optical-potential results of Khare, Kumar, and Lata [43] (100–800 eV, dashed curve *B*) compare reasonably well with the present and experimental data.

Also shown in Fig. 3 are the recent theoretical calculations of Nahar and Wadhera [44] (20–300 eV, curve *A*) who employed a complex-optical-potential approach treated under the phase-shift analysis. They [44] also produce the hump structure in the σ_t, however, their values are higher than the present and all other experimental values as shown in Fig. 3.

Figure 4 illustrates our positron-Kr σ_t cross sections along with experimental points of Coleman *et al.* [12] (200–960 eV, +), Dababneh *et al.* [21] (20–50 eV, open circles), and Dababneh *et al.* [24] (20–800 eV, crosses). No previous theoretical calculations could be found for this system. Our theoretical curve in Fig. 4 compares very well with the recent measurements of Dababneh *et al.* [21,24]. There is clearly a peaking behavior in σ_t around 30 eV. The measurements of Dababneh *et al.* [24] and Coleman *et al.* [12] differ significantly from each other at all energies. Our calculated numbers agree with the measurements of Dababneh *et al.* [21,24] within their experimental uncertainty (not shown). Nevertheless, the maximum difference between theory and experiment (Refs. [21] and [24]) is about 10% around the 40–60-eV region, which is less than the total estimated error in the experimental data [21,24].

In Fig. 5, we have shown our positron-Xe total cross sections along with experimental data of Canter *et al.* [8] (2–400 eV, +), Dababneh *et al.* [21] (0.5–100 eV, open

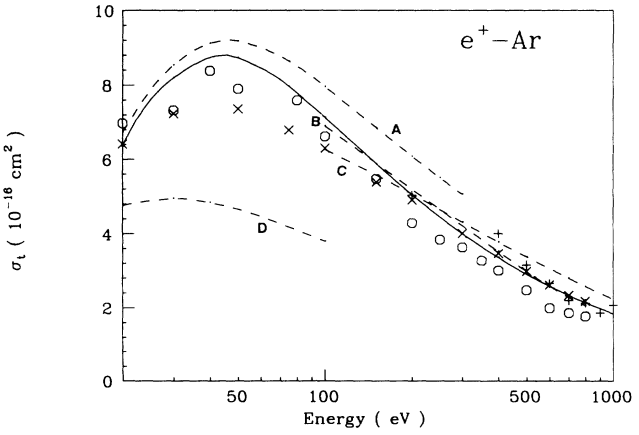

FIG. 3. Total cross sections for the positron-Ar scattering at 20–1000 eV. Calculations: solid line, present results; dashed curve *A*, calculations of Ref. [44]; dashed curve *B*, complex potential results of Ref. [43]; dashed curve *C*, optical model calculations of Ref. [40]); dashed curve *D*, optical potential results of Ref. [45]. Experimental data: ×, Kauppila *et al.* (Ref. [23]); ○, Griffith *et al.* (Ref. [19]); +, Brenton, Dutton, and Harris (Ref. [15]).

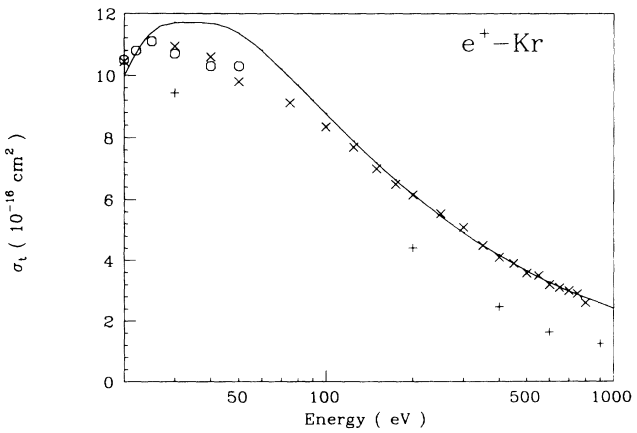

FIG. 4. Total cross sections for the positron-Kr case at 20–1000 eV. Solid curve is the present theory, while measurements are taken from Ref. [24] (×), [21] (○), and [12] (+).

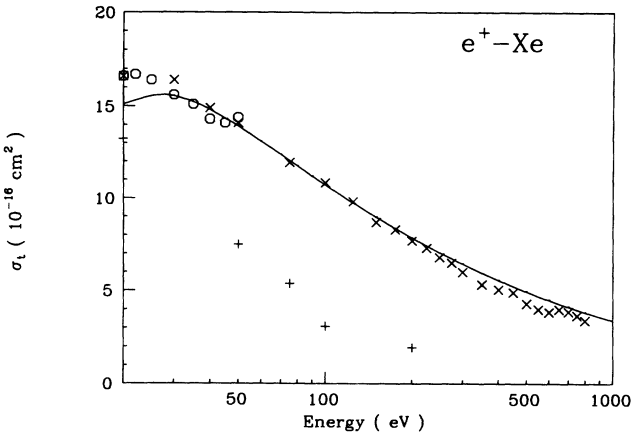

FIG. 5. Total cross sections for the positron-Xe system at 20–1000 eV. Present calculations are shown by solid curve. The experimental data are from Refs. [24] (×), [21] (○), and [8] (+).

circles), and Dababneh *et al.* [24] (20–800 eV, crosses). Our agreement with these measurements is very good at all energies except below 30 eV, where theory underestimates experiment by about 10%. However, this difference of 10% between theory and experiment is within experimental error bars (not shown). This is remarkable since we are not fitting our cross section at a particular energy. We have chosen only the form of the absorption potential [Eq. (10)] in an approximate way. The peaking behavior, as previously seen for He, Ne, and Ar atoms and to some extent for Kr atoms also, has almost disappeared for the Xe case in the present energy regime. In general, the intermediate-energy peak, occurring in the energy dependence of σ_t, shifts from higher energies to lower energies as we go from He to Xe atoms.

Finally, our predicted results for the positron-Rn system are plotted in Fig. 6. We are unaware of previous data, experimental or theoretical, that are available for this gas in order to compare with our curve in Fig. 6. A close look at the total cross sections for all the rare gases

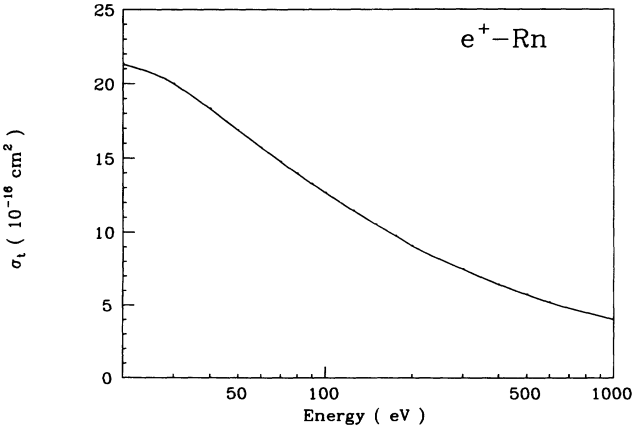

FIG. 6. Present predictions on the total cross sections for the positron-Rn system in the energy range of 20–1000 eV.

(Figs. 1–6) reveals some interesting facts. For example, the hump structure in the energy dependence of $\sigma_t(E)$ slowly moves towards lower energies as we go from helium to radon. In cases of helium and neon, the bell shape (peak occurring around 75 eV) of the σ_t curve is very pronounced. However, for the argon scattering (Fig. 3), the hump structure is weaker and occurs at somewhat lower energy (45 eV) as compared to the He and Ne cases. For the Kr case, the hump structure in the $\sigma_t(E)$ is even weaker. Finally for the heavier Xe and Rn gases, the energy dependence of $\sigma_t(E)$ is almost a monotonically decreasing function with energy in the present intermediate- and high-energy regions. This is consistent with experimental observation as well as with the change in ionization potential (and therefore the Ps threshold) of the target (see Table II). It seems that the peak in the σ_t curve occurs roughly at an energy which is almost three times higher than the respective ionization potential of the atom.

We now discuss the quality of our σ_t with respect to individual σ_{el} and σ_{abs} values. For the case of positron-He scattering, measured values of σ_{ion} and σ_{Ps} are available in the present energy range (Ref. [65]). The electronic excitation cross sections (σ_{exc}) have been calculated by Srivastava, Kumar, and Tripathi [66] for the dominant channels ($2\,^1S$ and $2\,^1P$) of the excited helium. In Fig. 7 we have plotted our σ_{abs} cross sections against the quantities $\sigma_{ion}+\sigma_{Ps}$ (both experimental [65]) and $\sigma_{ion}+\sigma_{Ps}+\sigma_{exc}$ (where σ_{exc} includes the $2\,^1S$ and $2\,^1P$ excited states). We can clearly see that our σ_{abs} are the upper limit of the sum of these individual terms. The good comparison in Fig. 7 between our calculated σ_{abs} and sum of all dominant inelastic cross sections has given us confidence in the choice of our absorption potential of Eq. (10). In order to see this success further for a heavier system, in the same Fig. 7, we have compared our

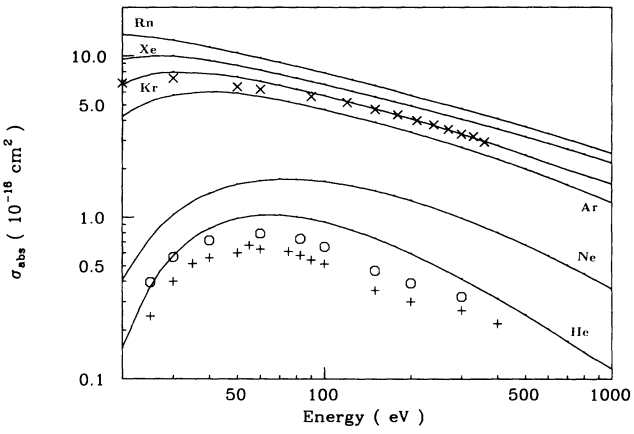

FIG. 7. Absorption (total inelastic) cross sections for the positron scattering with He, Ne, Ar, Kr, Xe, and Rn gases. The lower set of experimental points are the inelastic sum of Ref. [65] (+, $\sigma_{ion}+\sigma_{Ps}$). The open circles include electronic excitation ($2\,^1S+2\,^1P$) results for He from Ref. [66]. The upper set of points (×) are the inelastic cross sections for the positron-Kr system as discussed in Ref. [67].

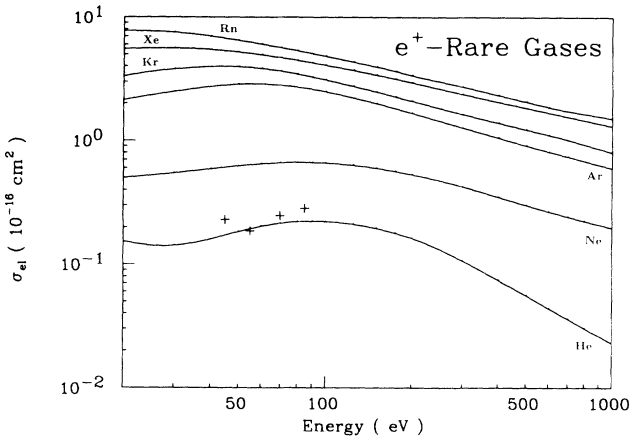

FIG. 8. Elastic (σ_{el}) cross sections for all the rare gases. The experimental points (+) are for the positron-He case taken from Ref. [68].

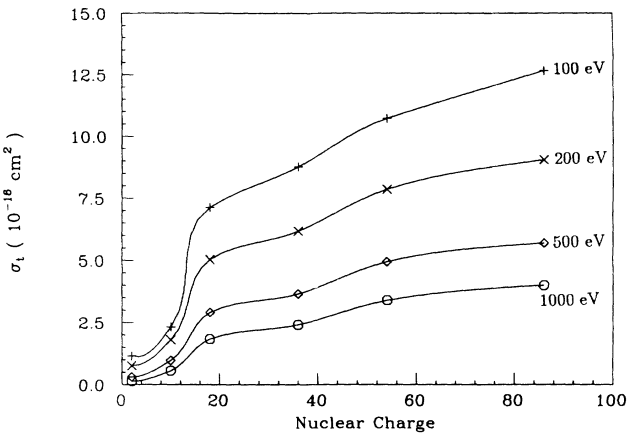

FIG. 9. A correlation diagram of σ_t with respect to number of target electrons (Z) at 100 eV (+), 200 eV (×), 500 eV (◇) and 1000 eV (○).

positron-Kr σ_{abs} values with the measured inelastic cross sections of Diana *et al.* [67]. It is rather surprising that our σ_{abs} are in excellent agreement, both in shape and magnitude, with measured inelastic cross sections [67]. Finally, in Fig. 7, we have shown our σ_{abs} values for all other rare gases in the present range of energy (20–1000 eV). These σ_{abs} can be useful in order to estimate total inelastic cross section for positron–rare-gas collisions.

In order to further see the quality of the σ_{el} parameter in the present model, we have shown σ_{el} values for all the rare gases in Fig. 8. For the He case, we have compared the present σ_{el} curve with experimental numbers of Diana [68]. Thus we see that our complex optical potential gives quite reliable results not only for the total cross sections but for the elastic and inelastic components as well.

IV. CORRELATION OF σ_t WITH MOLECULAR PARAMETERS

Very recently Szmytkowski [35] has discussed the trend relating experimental σ_t with the polarizability of the target. He has also noticed some correlation of total cross section with diamagnetic susceptibility and atomic number (Z) of the target. A similar analysis between σ_t and Z is given by Floeder *et al.* [70] for the case of positron scattering with hydrocarbon molecules. It will be interesting to correlate present σ_t with the target α_0 or Z and draw some definitive conclusions. First, in Fig. 9, we have plotted σ_t against Z at a few selected energies. In Fig. 10, we have plotted σ_t against α_0. From Figs. 9 and 10, we notice that σ_t increases with Z and α_0 but decreases with energy E. Beyond Ne, the variations are smooth. We made a multiterm least-squares fit to all the rare-gas data (except for He and Ne) beyond 100 eV in the form

$$\sigma_t(10^{-16}\ \text{cm}^2)=aZ^b[\alpha_0^c(\text{units of } a_0^3)][E^d(\text{eV})]\ , \qquad (22)$$

and obtained $a=21.65$, $b=-0.000\,33$, $c=0.559$, and $d=-0.5397$. This implied that σ_t is nearly proportional to $(\alpha_0/E)^{1/2}$ which is reminiscent of the formula given by Vogt and Wannier [71] for the scattering of ions by polarization forces. In Fig. 11, we have shown $\sigma_t(E/\alpha_0)^{1/2}$ against Z for all values of E above 100 eV. We notice that for heavier gases, $\sigma_t(E/\alpha_0)^{1/2}$ becomes almost independent of the nuclear charge. The correlation of σ_t and α_0 becomes progressively stronger as we go from Ar to Rn. It seems that for systems having $\alpha_0 \geq \alpha_0(\text{Rn})$, the correlation will be even more dominant.

Encouraged by Fig. 11 and the general form [Eq. (22)], we have fitted a simple formula,

$$\sigma_t(10^{-16}\ \text{cm}^2)=21.16\left[\frac{[\alpha_0(\text{units of } a_0^3)]}{E(\text{eV})}\right]^{1/2}. \qquad (23)$$

The fitted cross sections [Eq. (23)] with respect to input σ_t are shown in Fig. 12 for Ar, Kr, Xe, and Rn gases. We see that the above formula works very well for these relatively heavier gases. However, the fit is not that good for He and Ne targets whose polarizabilities are quite small.

It is quite interesting that Eq. (23) can give a very good estimate of σ_t for a large number of other atomic and

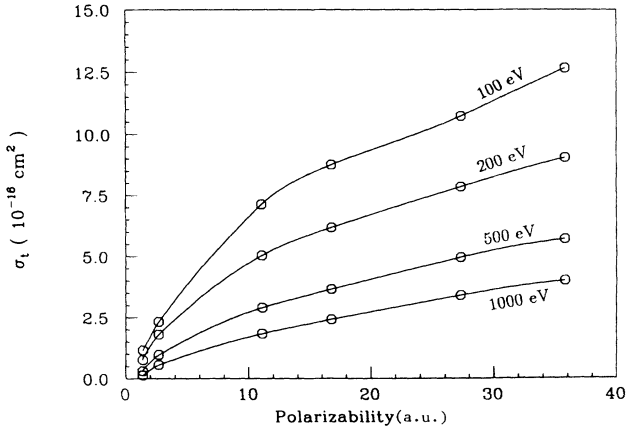

FIG. 10. A correlation diagram between σ_t target polarizability (α_0) at various energies.

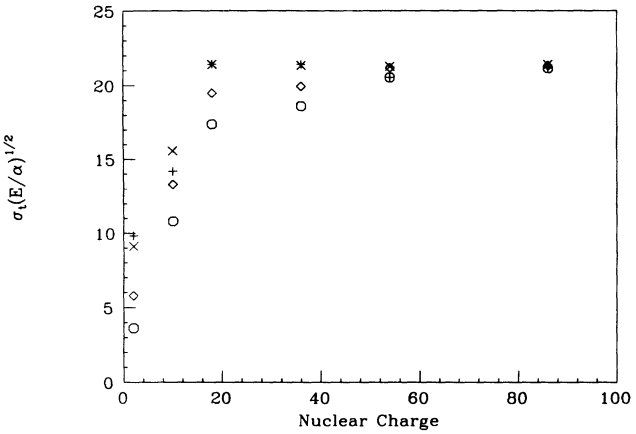

FIG. 11. Same caption as in Fig. 9 except between $\sigma_t(E/\alpha_0)^{1/2}$ and Z.

molecular targets (see next section). The role of polarizability in shaping up the intermediate- and high-energy positron-target total cross section is not very clear at this time. The form [Eq. (23)] of σ_t is quite similar (except the normalization constant) to the one discussed by Nishimura and Tawara [72]. However, in the present model, we have included short-range repulsive force as well as the absorption potential [Eq. (10)] in order to obtain present σ_t values. Therefore it seems that relation [Eq. (23)] is purely on an empirical basis, but a quite useful one.

σ_t for highly polarizable atomic and molecular systems using Eq. (23)

We would like to see the predictive power of our simple formula [Eq. (23)] for σ_t in terms of α_0 for other atomic and molecular systems whose polarizabilities are quite large. For example, σ_t have been measured for highly polarizable alkali-metal atoms (Na, K, Rb) at intermediate energies (1–100 eV) [49,69]. In addition, positron total cross sections have also been measured for several hydrocarbon molecules [70,73,74] (C_2H_4, C_2H_6, C_3H_6, C_6H_6, etc.) and other big molecules [75] (e.g., SF_6). It is to be noted here that no previous theoretical calculations are available for these big molecules whose polarizabilities are very large.

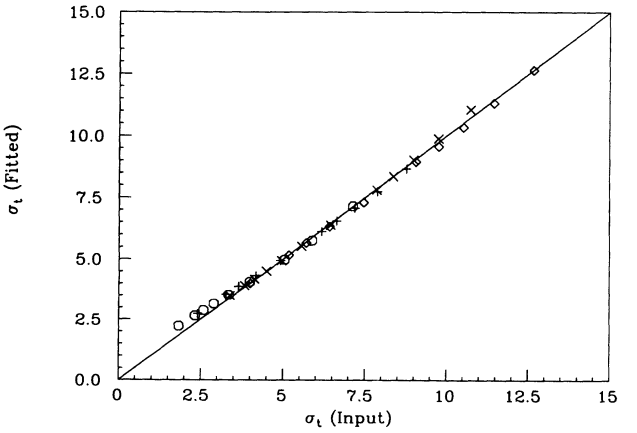

FIG. 12. σ_t (calculated) vs σ_t [fitted as in Eq. (22)] for the case of Ar (○), Kr (+), Xe (×), and Rn (◇).

First, we show our σ_t [using the formula of Eq. (23)] for C_2H_4 ($\alpha_0=28.7a_0^3$), C_2H_6 ($\alpha_0=30.17a_0^3$), and C_3H_6 ($\alpha_0=38.20a_0^3$) molecules in Figs. 13(a)–13(c) along with experimental data from Refs. [70,73]. We see that the simple relation [Eq. (23)] between σ_t and α_0 can yield very accurate cross sections for such big molecules in the present energy region. The maximum difference between theory and experiment for σ_t using Eq. (23) is still less

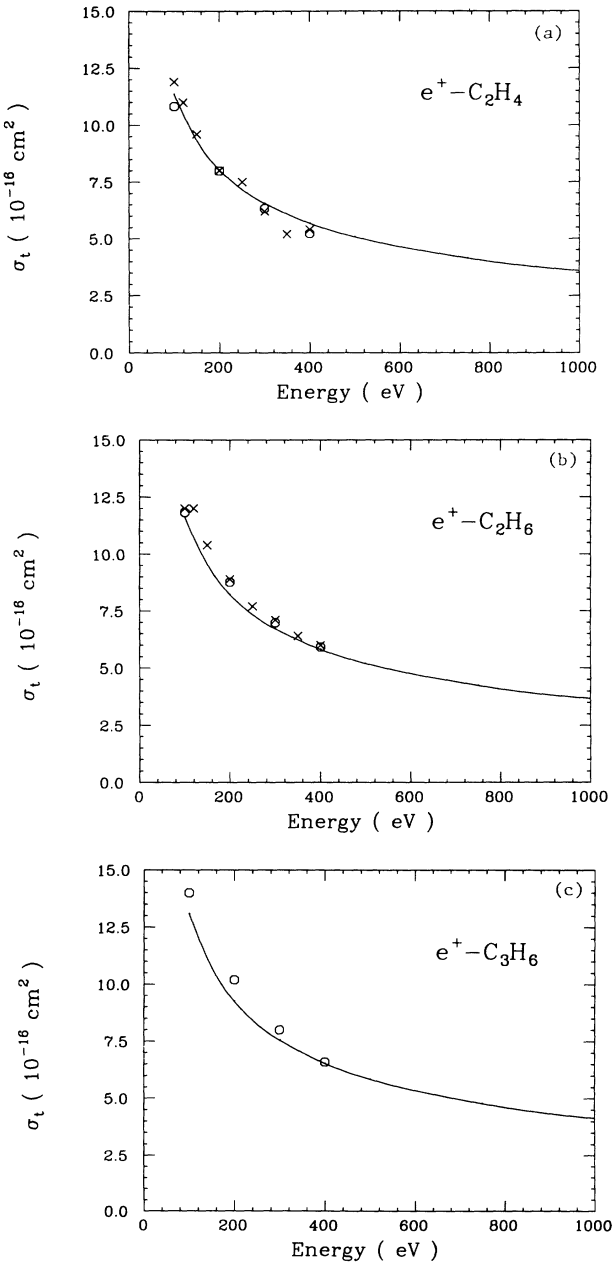

FIG. 13. Total cross sections for several hydrocarbon molecules by employing the formula given in Eq. (23). (a) C_2H_4, (b) C_2H_6, and (c) C_3H_6. The experimental points in all these curves are taken from Refs. [71] (×) and [70] (○).

than the experimental uncertainty.

We now use Eq. (23) to predict σ_t for Na ($\alpha_0=159.27a_0^3$), K ($\alpha_0=292.9a_0^3$), and Rb ($\alpha_0=319.23a_0^3$) alkali-metal atoms in the energy range of 10–100 eV where recent experimental data [49,69] are available. Figures 14(a)–14(c) illustrate our results along with measured points for Na, K, and Rb targets, respectively. To our surprise, the agreement between experiment and our derived formula [Eq. (23)] for σ_t is excellent except for the lighter Na atom where this agreement is only fair. It is well known that the positron scattering with alkali-metal atoms is quite complicated due to the fact that all the channels (elastic, Ps formation, electronic excitation, and ionization) are strongly coupled even at very low energies. In their five-state close-coupling calculations on the positron-Na system, Ward *et al.* [76] could include only elastic and few excitation channels and neglected Ps formation and ionization processes, which are important at low energy (below roughly 10 eV) and may be small at higher energies. The agreement of experimental total cross sections for Na and K atoms with several calculations [77–84] (this reference list is not complete), as discussed by Kwan *et al.* [49], is only satisfactory.

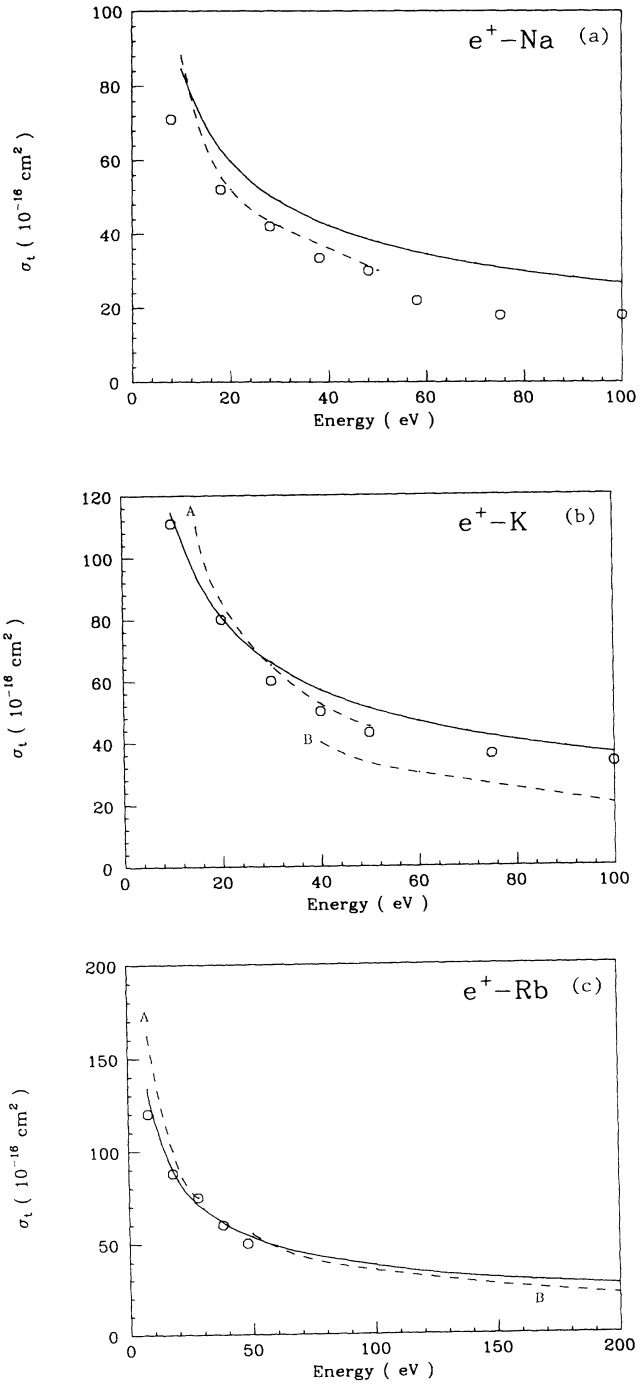

FIG. 14. Total cross sections for several alkali-metal atoms by employing the formula given in Eq. (23). (a) Na, (b) K, and (c) Rb. The experimental points (○) in all these curves are taken from Refs. [49] (Na and K) and [69] (Rb). The dashed curves: (a) theoretical values of Ward *et al.* (Ref. [76]); (b) calculations of Gien (Ref. [79]) (curve *B*) and Ward *et al.* (Ref. [76]) (curve *A*); (c) calculations of McEachran *et al.* (Ref. [83]) (curve *A*) and Gien (Ref. [81]) (curve *B*).

Our estimated values for the positron-K system obtained from Eq. (23) are shown in Fig. 14(b) along with measurements of Stein *et al.* [85] and calculations of Refs. [78] and [79]. We can see from Fig. 14(b) that Eq. (23) gives very accurate total cross-section values for the positron-K scattering system from low (10 eV) to intermediate energies. For the positron-Rb case, our σ_t values obtained from Eq. (23) are shown in Fig. 14(c) along with experimental points from Ref. [49] and the close-coupling calculations of McEachran *et al.* [83] (neglecting Ps formation and ionization channels). In Fig. 14(c), we have also included a very recent modified Glauber (MG) calculation of Gien [84]. We see that the present results employing Eq. (23) are much better than previous calculations when compared with measured cross sections.

Thus the usefulness of our simple σ_t formula [Eq. (23)] is clear: in the absence of theoretical data for any particular target with large polarizability, Eq. (23) can give a very good estimate of the σ_t parameter in a wide energy range. We have demonstrated this for several molecular and atomic systems in Figs. 13 and 14.

V. CONCLUDING REMARKS

We have presented total cross sections for positron scattering with all the rare gases in the energy range of 20–1000 eV. A complex-optical-potential approach is employed in which the real part is included correctly at the Dirac-Hartree-Fock level, while the form of imaginary part is derived semiempirically. There is no adjustable parameter involved in the present model except the choice of the approximate form [Eq. (10)] of the absorption potential as mentioned above. We are able to reproduce experimental σ_t (within experimental uncertainty) for all the rare gases in the present energy regime. We also found a strong correlation between σ_t and the polarizability of the target (see Ref. [71] for the electron case). A simple analytical formula [Eq. (23)] relating $\sigma_t(E)$ and

α_0 is derived. It is found that this correlation (σ_t and α_0) is more pronounced for targets with large polarizability. Our simple formula [Eq. (23)] is shown to work very well for several hydrocarbon molecules and alkali metals whose polarizabilities are very large. We emphasize that Eq. (23) can be used safely for those highly polarizable targets where no previous results on the σ_t are available for comparison.

ACKNOWLEDGMENTS

This research is funded by the Research Corporation, Tuscon, Arizona under Contract No. C-2924. This work is also partially supported by the U.S. Army Office of Scientific Research under Contract No. DAAL03-89-9-0111.

*Permanent address: Department of Physics and Astrophysics, University of Delhi, Delhi 110 007, India.

[1] D. G. Costello, D. E. Groce, D. F. Herring, and J. Wm. McGowan, Can. J. Phys. **50**, 23 (1972).
[2] K. F. Canter, P. G. Coleman, T. C. Griffith, and G. R. Heyland, J. Phys. B **5**, L167 (1972).
[3] B. Jaduszliwer and D. A. L. Paul, Can. J. Phys. **51**, 1565 (1973).
[4] K. F. Canter, P. G. Coleman, T. C. Griffith, and G. R. Heyland, J. Phys. B **6**, L201 (1973).
[5] B. Jaduszliwer and D. A. L. Paul, Appl. Phys. **3**, 281 (1974).
[6] B. Jaduszliwer and D. A. L. Paul, Can. J. Phys. **52**, 272 (1974).
[7] B. Jaduszliwer and D. A. L. Paul, Can. J. Phys. **52**, 1047 (1974).
[8] K. F. Canter, P. G. Coleman, T. C. Griffith, and G. R. Heyland, Appl. Phys. **3**, 249 (1974).
[9] B. Jaduszliwer, A. Nakashima, and D. A. L. Paul, Can. J. Phys. **53**, 962 (1975).
[10] J. Dutton, F. M. Harris, and R. A. Jones, J. Phys. B **8**, L65 (1975).
[11] J. S. Tsai, L. Lebow, and D. A. L. Paul, Can. J. Phys. **54**, 1741 (1976).
[12] P. G. Coleman, T. C. Griffith, G. R. Heyland, and T. R. Twomey, Appl. Phys. **11**, 321 (1976).
[13] W. E. Kauppila, T. S. Stein, and G. Jesion, Phys. Rev. Lett. **36**, 580 (1976).
[14] J. R. Burciaga, P. G. Coleman, L. M. Diana, and J. D. McNutt, J. Phys. B **10**, L569 (1977).
[15] A. G. Brenton, J. Dutton, and F. M. Harris, J. Phys. B **11**, L15 (1978).
[16] T. S. Stein, W. E. Kauppila, V. Pol, J. H. Smart, and G. Jesion, Phys. Rev. A **17**, 1600 (1978).
[17] W. E. Wilson, J. Phys. B **11**, L629 (1978).
[18] P. G. Coleman, J. D. McNutt, L. M. Diana, and J. R. Burciaga, Phys. Rev. A **20**, 145 (1979).
[19] T. C. Griffith, G. R. Heyland, K. S. Lines, and T. R. Twomey, Appl. Phys. **19**, 431 (1979).
[20] P. G. Coleman, J. D. McNutt, L. M. Diana, and J. T. Hutton, Phys. Rev. A **22**, 2290 (1980).
[21] M. S. Dababneh, W. E. Kauppila, J. P. Downing, F. Laperriere, V. Pol, J. H. Smart, and T. S. Stein, Phys. Rev. A **22**, 1872 (1980).
[22] G. Sinapius, W. Raith, and W. G. Wilson, J. Phys. B **13**, 4079 (1980).
[23] W. E. Kauppila, T. S. Stein, J. H. Smart, M. S. Dababneh, Y. K. Ho, J. P. Downing, and V. Pol, Phys. Rev. **24**, 725 (1981).
[24] M. S. Dababneh, Y. F. Hseih, W. E. Kauppila, V. Pol, and T. S. Stein, Phys. Rev. A **26**, 1252 (1982).
[25] M. Charlton, G. Laricchia, T. C. Griffith, G. L. Wright, and G. R. Hegland, J. Phys. B **17**, 4945 (1984).
[26] T. Mizogawa, Y. Nakayama, T. Kawaratani, and M. Tosaki, Phys. Rev. A **31**, 2171 (1985).
[27] T. C. Griffith and G. R. Heyland, Phys. Rep. **39C**, 169 (1978).
[28] T. C. Griffith, Adv. At. Mol. Phys. **15**, 135 (1979).
[29] W. E. Kauppila and T. S. Stein, Can. J. Phys. **60**, 471 (1982).
[30] T. S. Stein and W. E. Kauppila, Adv. At. Mol. Phys. **18**, 53 (1982).
[31] W. Raith, in *Positron Scattering in Gases,* edited by J. W. Humberston and M. R. C. McDowell (Plenum, New York, 1984), pp. 1–13.
[32] M. Charlton, Rep. Prog. Phys. **48**, 737 (1985).
[33] T. C. Griffith, Adv. At. Mol. Phys. **22**, 37 (1986).
[34] T. S. Stein and W. E. Kauppila, in *Electronic and Atomic Collisions,* edited by D. C. Lorentz *et al.* (Elsevier, New York, 1986), p. 105.
[35] C. Szmytkowski, Z. Phys. D **13**, 69 (1989).
[36] C. J. Joachain, K. H. Winters, and F. W. Byron, J. Phys. B **8**, 289 (1975).
[37] D. P. Dewangen and H. R. J. Walters, J. Phys. B **10**, 637 (1977).
[38] F. W. Byron and C. J. Joachain, Jr., Phys. Rev. A **15**, 128 (1977).
[39] F. W. Byron, Phys. Rev. A **17**, 170 (1978).
[40] C. J. Joachain, R. Vanderpportens, K. H. Winters, and F. W. Byron, J. Phys. B **10**, 227 (1977).
[41] T. T. Gien, as quoted in Ref. [23].
[42] K. Lata, Ph.D. thesis, Meerut University, India, 1984.
[43] S. P. Khare, Ashok Kumar, and Kusum Lata, Phys. Rev. A **33**, 2795 (1986).
[44] S. N. Nahar and J. M. Wadhera, Phys. Rev. A **43**, 1275 (1987).
[45] K. Bartschat, R. P. McEachran, and A. D. Stauffer, J. Phys. B **21**, 2789 (1988).
[46] K. Bartschat, R. P. McEachran, and A. D. Stauffer, J. Phys. B **23**, 2349 (1990).
[47] F. W. Byron and C. J. Joachain, Phys. Rep. **34**, 233 (1977).
[48] H. R. J. Walters, Phys. Rep. **116**, 1 (1984).
[49] C. K. Kwan, W. E. Kauppila, R. A. Lukaszew, S. P. Parikh, T. S. Stein, Y. J. Wan, and M. S. Dababneh, Phys. Rev. A **44**, 1620 (1991).
[50] O. Sueoka, in *Atomic Physics With Positrons,* edited by J. W. Huberston and E. A. G. Armour (Plenum, New York, 1987), p. 41.
[51] K. L. Baluja and A. Jain, Phys. Rev. A **45**, 202 (1992).
[52] C. J. Joachain, *Quantum Collision Theory* (North-Holland, New York, 1984).
[53] A. Jain, Phys. Rev. A **41**, 2437 (1990).

[54] A. Jain, NASA Report No. C-3058, 1990 (unpublished).
[55] A. Jain, J. Phys. B **23**, 863 (1991).
[56] G. Staszewska, D. W. Schwenke, D. Thirumalai, and D. G. Truhlar, J. Phys. B **16**, L281 (1983); Phys. Rev. A **28**, 2740 (1983); G. Staszewska, D. W. Schwenka, and D. G. Truhlar, J. Chem. Phys. **81**, 335 (1984); Phys. Rev. A **29**, 3078 (1984).
[57] F. Calogero, *Variable Phase Approach to Potential Scattering* (Academic, New York, 1974).
[58] C. Froese-Fischer, *The Hartree-Fock Method for Atoms* (Wiley, New York, 1977).
[59] A. Jain, B. Etemadi, and K. R. Karim, Phys. Scr. **41**, 321 (1990).
[60] F. Salvat, J. D. Martinez, R. Mayol, and J. Parellada, Phys. Rev. A **36**, 467 (1987).
[61] See C. J. Joachain and R. M. Potvliege, Phys. Rev. A **35**, 4873 (1987).
[62] M. Inokuti, Y. K. Kim, and R. L. Platzman, Phys. Rev. **164**, 55 (1967).
[63] M. Inokuti and M. R. C. McDowell, J. Phys. B **7**, 2382 (1974).
[64] R. P. Saxon, Phys. Rev. A **8**, 839 (1973).
[65] D. Fromme, G. Kruse, W. Raith, and G. Sinapius, J. Phys. B **21**, L261 (1988).
[66] R. Srivastava, M. Kumar, and A. N. Tripathi, in *Positron (Electron)-Gas Scattering,* edited by Kauppila *et al.* (World Scientific, Singapore, 1986), p. 273.
[67] L. M. Diana, P. G. Coleman, D. L. Brooks, and R. L. Chaplin, in *Atomic Physics with Positrons* (Ref. [50]), p. 55.
[68] L. M. Diana (private communication).
[69] T. S. Stein, W. E. Kauppila, C. K. Kwan, R. A. Lukaszew, S. P. Parikh, Y. J. Wan, S. Zhou, and M. S. Dababneh, in Ref. [54].
[70] K. Floeder, D. Fromme, W. Raith, A. Schwab, and G. Sinapius, J. Phys. B **18**, 3347 (1985).
[71] E. Vogt and G. H. Wannier, Phys. Rev. **95**, 1190 (1954).
[72] H. Nishimura and H. Tawara, J. Phys. B **24**, L363 (1991).
[73] O. Sueoka and S. Mori, J. Phys. B **19**, 4035 (1986).
[74] O. Sueoka, J. Phys. B **21**, L631 (1988).
[75] M. S. Dababneh, Y. F. Hsieh, W. E. Kauppila, C. K. Kwan, S. J. Smith, T. S. Stein, and M. N. Uddin, Phys. Rev. A **38**, 1207 (1988).
[76] S. J. Ward, M. Horbatsch, R. P. McEachran, and A. D. Stauffer, J. Phys. B **22**, 1845 (1989).
[77] K. P. Sarkar, M. Basu, and A. S. Ghosh, J. Phys. B **21**, 1649 (1988).
[78] S. J. Ward, M. Horbatsch, R. P. McEachran, and A. D. Stauffer, J. Phys. B **21** L611 (1988).
[79] T. T. Gien, Phys. Rev. A **35**, 2026 (1987).
[80] T. T. Gien, J. Phys. B **22**, L463 (1988).
[81] T. T. Gien, J. Phys. B **22**, L129 (1988).
[82] S. P. Khare and X. Vijayshri, Ind. J. Phys. **61B**, 404 (1987).
[83] R. P. McEachran, M. Horbatsch, A. D. Stauffer, and S. J. Ward, in Ref. [54].
[84] T. T. Gien, Phys. Rev. A **44**, 5693 (1991).
[85] T. S. Stein, M. S. Dababneh, W. E. Kauppila, C. W. Kwan, and Y. J. Wan, in *Atomic Physics with Positrons* (Ref. [50]), p. 251.